VIBRATION AND BUCKLING CHARACTERISTICS OF COMPOSITE CYLINDRICAL PANELS INCORPORATING THE EFFECTS OF A HIGHER ORDER SHEAR THEORY

A. N. Palazotto and Peter E. Linnemann

Air Force Institute of Technology, Wright-Patterson AFB, OH 45433, U.S.A.

Abstract—An analytical study is conducted to determine the fundamental frequencies and critical buckling loads for laminated anisotropic circular cylindrical shell panels, including the effects of transverse shear deformation and rotary inertia, by using the Galerkin technique. A linearized form of Sander's shell strain–displacement relations are derived, which include a parabolic distribution of transverse shear strains. The theory is valid for laminate thickness to radius ratios, h/R, of up to 1/5. Higher order constitutive relations are derived for the laminate. A set of five coupled partial differential equations of motion and boundary conditions are derived and then solved using the modified Galerkin technique. Simply supported and clamped boundary conditions are investigated. Comparisons are made with the Donnell shell solutions. The effects of transverse shear deformation and rotary inertia are examined by comparing the results with classical solutions, where applicable. The radius of curvature is varied to determine the effects of membrane and bending coupling. The theory compares exactly with the Donnell solutions, which are valid up to $h/R = 1/50$. As expected, as length to thickness ratios are reduced, shear deformation effects significantly lower the natural frequencies and buckling loads. Analysis also shows that rotary inertia effects are very small. Finally, as h/R is varied from 0 (flat plate) to 1/5 (maximum limit), the frequencies and buckling loads increase due to membrane and bending coupling.

INTRODUCTION

Because of the potentially large spatial variations of stiffness properties in composite shell structures due to tailoring, three-dimensional stress and strain effects become very important. Whereas classical two-dimensional assumptions may be valid for an identical shell structure consisting of isotropic materials, they may lead to gross inaccuracies for an orthotropic construction (Dennis and Palazotto, 1989, 1990).

Past research has clearly indicated the need to refine the classical Kirchhoff–Love shell theories to better predict the stability and dynamic responses of composite cylindrical shell configurations. The Kirchhoff–Love theory assumes normals to the shell mid-surface before deformation remain normal after deformation, effectively neglecting transverse shear strains. These classical theories predict shell panels that are too stiff, resulting in high frequencies and buckling loads. L. H. Donnell applied the Kirchhoff–Love theory to cylindrical shell panels. The need to include transverse shear effects was first recognized by Reissner (1945), followed by Mindlin (1951), who included rotary inertia effects in the dynamic analysis of plates. The Reissner–Mindlin theory assumes the cross-section remains plane, but is allowed to rotate from the normal with respect to the mid-surface after deformation. Additional independent degrees of freedom are included, which enables the transverse shear to be fully described by the shell mid-surface degrees of freedom and the thickness coordinate. This first order theory does not satisfy the boundary conditions of zero transverse shear on the top and bottom surfaces of the laminate because of the constant shear angle assumed. The introduction of a correction factor helps to alleviate this problem.

Reddy (1984a,b), Reddy and Liu (1985) and Soldatos (1987) have recently applied a so-called parabolic through the thickness shear strain distribution to analyze laminated anisotropic plates and shells. The in-plane displacements are cubic functions of the thickness coordinate, satisfying zero transverse shear strain boundary conditions on the top and bottom surfaces of the laminate. The same independent degrees of freedom as used in Reissner–Mindlin theory are used here, but the need for a correction factor is eliminated.

In light of the above, this paper focuses on the fundamental natural frequencies of vibration and the critical buckling loads of symmetrically placed laminated composite circular cylindrical shell panels including the following:

(1) Linear displacement and rotations, and linear elastic behavior of cylindrical shells.
(2) Parabolic transverse shear strain and stress modeling.
(3) Bifurcation buckling analysis.
(4) Harmonic vibration analysis excluding transients.
(5) Analytical solution method using the Galerkin technique.

There are four main objectives to this paper. First is the development of a higher order set of linear strain–displacement relations for the cylindrical panel that incorporate parabolic transverse shear. The relations could be regarded as a linearized form of Sanders equations, applicable to deep panels (almost complete cylinders). The theory is not limited to shallow panels as is Donnell theory as pointed out by Bert and Kumar (1982). In fact, this last reference considers not only the Sanders and Donnell approximation but also the Loo, Love and Morley type shell approximations. The strain–displacement relations result in higher order constitutive relations for the panel. The second objective is the analytical solution for the fundamental frequencies and critical buckling loads of the cylindrical panel for different geometries and boundary conditions. Third, the method will be used to analyze the effects of shear deformation, rotary inertia, and radius of curvature. Intrinsic in this analysis is the determination of the maximum thickness to radius ratio allowed under the conditions of assuming zero transverse normal stress. The fourth objective of the paper is verification of the results by comparison with other approximate methods and classical methods, where applicable.

FORMULATION

The coordinate system for the circular cylindrical shell panel and the degrees of freedom are shown in Fig. 1. The x and y axes are located at the mid-surface of the laminate ($z = 0$). The degrees of freedom $u_0(x,y,t)$, $v_0(x,y,t)$, and $w(x,y,t)$ are the laminate mid-surface displacements in the x, y, and z directions, respectively. The degrees of freedom $\psi_x(x,y,t)$ and $\psi_y(x,y,t)$ are the rotations of the laminate cross-section from the normal at the mid-surface with respect to the y and x axes, respectively. R is the radius of curvature, h the laminate thickness, a the length in the x direction, and b the length in the y direction.
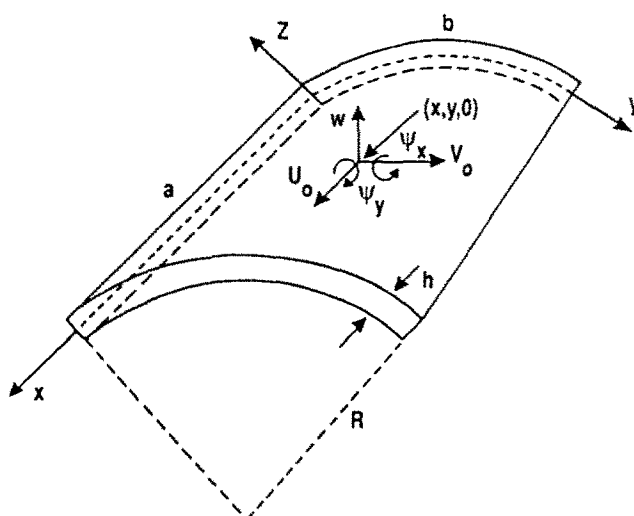

Fig. 1. Shell panel coordinates and degrees of freedom.

In order to determine the displacement field, the transverse shear strains, γ_{xz} and γ_{yz}, need to be modeled. In classical laminated shell theory, through the thickness shear deformation is neglected according to the Kirchhoff–Love hypothesis that plane cross-sections remain plane and perpendicular to the laminate mid-surface after deformation. A displacement field that is a first order function of x is required in classical shell theory. Bowlus et al. (1985, 1987) and Palardy and Palazotto (1990) in their flat plate work modeled transverse shear strain using Mindlin plate theory, which also required the use of a first order displacement field. Mindlin plate theory assumes the cross-section remains plane, but is allowed to rotate from the normal with respect to the mid-surface after deformation. The assumption of no cross-sectional warping introduces error, especially at the top and bottom surfaces of the laminate, since the model does not match the boundary conditions of zero transverse shear strain there. This error is reduced by the introduction of a shear correction factor. This paper models transverse shear strain parabolically wherein the strains are maximum at the laminate mid-surface and are zero at the top and bottom surfaces, satisying the boundary conditions.

To achieve the desired parabolic transverse shear, a higher order displacement field is required, as opposed to the first order displacement field used in the Classical and Mindlin cases. The coordinate displacements in the x and y directions, u and v, will be constant with respect to z. From Reddy and Liu (1985), the generalized displacement field is:

$$u(x,y,z,t) = u_0 + z\psi_x + z^2\phi_1 + z^3\Theta_1$$

$$v(x,y,z,t) = \left(1 + \frac{z}{R}\right)v_0 + z\psi_y + z^2\phi_2 + z^3\Theta_2$$

$$w(x,y,t) = w \tag{1}$$

where $\phi_1, \phi_2, \Theta_1,$ and Θ_2 will be chosen to satisfy the boundary conditions of zero transverse shear strain at the laminate top and bottom surfaces.

Linear orthogonal curvilinear coordinates are used to develop the strain–displacement relations (Reddy and Liu, 1985; Saada, 1974) for a circular cylindrical shell panel, yielding the Donnell-type cylindrical shell equations.

The Donnell cylindrical shell panel equations assume $z/R \approx 0$. As shown subsequently this assumption limits Donnell theory to be valid only for small h/R ratios. With no transverse shear, the maximum h/R limit under Donnell assumptions is approximately $1/500$ (Whitney, 1984). As will be shown, with transverse shear included, the Donnell-type equations are valid up to h/R equal to approximately $1/50$ (Reddy and Liu, 1985).

For simplicity this paper assumes $z/R \ll 1$ only for the transverse shear strains, γ_{xz} and γ_{yz}; for the membrane strains ε_x, ε_y, and γ_{xy}, the following polynomial expansion is made:

$$\frac{1}{1 + \dfrac{z}{R}} \cong 1 - \frac{z}{R}. \tag{2a}$$

This approximation allows the strain–displacement relations to be valid for deep panels, with an h/R maximum limit of approximately $1/5$ (see Dennis and Palazotto, 1989, 1990). The transverse shear strains become:

$$\gamma_{yz} = v_{,z} + w_{,y} - \frac{v}{R}$$

$$\gamma_{xz} = u_{,z} + w_{,x}. \tag{2b}$$

if one sets $\gamma_{xz}(x,y,\pm h/2,t) = 0$ and $\gamma_{yz}(x,y,\pm h/2,t) = 0$ to satisfy the laminate surface boundary conditions, then from eqn (1) it can be shown that:

$$\phi_1 = \phi_2 = 0$$

$$\Theta_1 = k(\psi_x + w_{,x}), \quad \Theta_2 = k(\psi_y + w_{,y}) \tag{2c}$$

where $k = -4/3h^2$. The displacement field becomes:

$$u(x, y, z, t) = u_0 + z\psi_x + z^3 k(\psi_x + w_{,x})$$

$$v(x, y, z, t) = \left(1 + \frac{z}{R}\right)v_0 + z\psi_y + z^3 k(\psi_y + w_{,y})$$

$$w(x, y, z, t) = w. \tag{3}$$

Using this displacement field in the Sanders-type equations, the strain–displacement relations become:

$$\varepsilon_x = u_{0,x} + z\psi_{x,x} + z^3 k(\psi_{x,x} + w_{,xx})$$

$$\varepsilon_y = v_{0,y} + \frac{w}{R} + z\psi_{y,y} - \frac{1}{R}z^2\psi_{y,y} + z^3 k(\psi_{y,y} + w_{,yy}) - \frac{1}{R}z^4 k(\psi_{y,y} + w_{,yy})$$

$$\gamma_{xy} = u_{0,y} + v_{0,x} + z\left(\psi_{x,y} + \psi_{y,x} + \frac{1}{2R}(v_{0,x} - u_{0,y})\right)$$

$$\qquad - \frac{1}{R}z^2\psi_{y,x} + z^3 k(\psi_{x,y} + \psi_{y,x} + 2w_{,xy}) - \frac{1}{R}z^4 k(\psi_{y,x} + w_{,xy})$$

$$\gamma_{yz} = \psi_y + w_{,y} + 3kz^2(\psi_y + w_{,y})$$

$$\gamma_{xz} = \psi_x + w_{,x} + 3kz^2(\psi_x + w_{,x}) \tag{4}$$

(where in the γ_{yz} equation terms including v_0/R are taken to be higher order).

A shorthand notation can be introduced to rewrite the strains as follows:

$$\begin{Bmatrix} \varepsilon_x \\ \varepsilon_y \\ \gamma_{xy} \\ \gamma_{yz} \\ \gamma_{xz} \end{Bmatrix} = \begin{Bmatrix} \varepsilon_x^0 \\ \varepsilon_y^0 \\ \gamma_{xy}^0 \\ \gamma_{yz}^0 \\ \gamma_{xz}^0 \end{Bmatrix} + z\begin{Bmatrix} \kappa_x^0 \\ \kappa_y^0 \\ \kappa_{xy}^0 \\ 0 \\ 0 \end{Bmatrix} + z^2\begin{Bmatrix} \kappa_x^1 \\ \kappa_y^1 \\ \kappa_{xy}^1 \\ \kappa_{yz}^1 \\ \kappa_{xz}^1 \end{Bmatrix} + z^3\begin{Bmatrix} \kappa_x^2 \\ \kappa_y^2 \\ \kappa_{xy}^2 \\ 0 \\ 0 \end{Bmatrix} + z^4\begin{Bmatrix} 0 \\ \kappa_y^3 \\ \kappa_{xy}^3 \\ 0 \\ 0 \end{Bmatrix}. \tag{5}$$

(Note the superscripts on the κ terms are *not* exponents. They are for identification purposes only and simply distinguish among the high and low order curvature terms.) The strains at the laminate mid-surface are:

$$\begin{Bmatrix} \varepsilon_x^0 \\ \varepsilon_y^0 \\ \gamma_{xy}^0 \\ \gamma_{yz}^0 \\ \gamma_{xz}^0 \end{Bmatrix} = \begin{Bmatrix} u_{0,x} \\ v_{0,y} + \dfrac{w}{R} \\ u_{0,y} + v_{0,x} \\ \psi_y + w_{,y} \\ \psi_x + w_{,x} \end{Bmatrix} \tag{6}$$

and the curvature terms (κ) due to bending and shear deformation are defined as follows:

$$\begin{Bmatrix} \kappa_x^0 \\ \kappa_y^0 \\ \kappa_{xy}^0 \end{Bmatrix} = \begin{Bmatrix} \psi_{x,x} \\ \psi_{y,y} \\ \psi_{x,y} + \psi_{y,x} + \dfrac{1}{2R}(v_{0,x} - u_{0,y}) \end{Bmatrix}$$

$$\begin{Bmatrix} \kappa_y^1 \\ \kappa_{xy}^1 \\ \kappa_{yz}^1 \\ \kappa_{xz}^1 \end{Bmatrix} = \begin{Bmatrix} -\dfrac{1}{R}\psi_{y,y} \\ -\dfrac{1}{R}\psi_{x,y} \\ 3k(\psi_y + w_{,y}) \\ 3k(\psi_x + w_{,x}) \end{Bmatrix}$$

$$\begin{Bmatrix} \kappa_x^2 \\ \kappa_y^2 \\ \kappa_{xy}^2 \end{Bmatrix} = \begin{Bmatrix} k(\psi_{x,x} + w_{,xx}) \\ k(\psi_{y,y} + w_{,yy}) \\ k(\psi_{x,y} + \psi_{y,x} + 2w_{,xy}) \end{Bmatrix}$$

$$\begin{Bmatrix} \kappa_y^3 \\ \kappa_{xy}^3 \end{Bmatrix} = \begin{Bmatrix} -\dfrac{1}{R}k(\psi_{y,y} + w_{,yy}) \\ -\dfrac{1}{R}k(\psi_{x,y} + w_{,xy}) \end{Bmatrix}. \tag{7}$$

It is now possible to relate the laminate constitutive relationships in terms of the composite laminate coordinates using the terminology from Jones (1975):

$$\begin{Bmatrix} \sigma_x \\ \sigma_y \\ \tau_{xy} \end{Bmatrix}_k = \begin{bmatrix} \bar{Q}_{11} & \bar{Q}_{12} & \bar{Q}_{16} \\ \bar{Q}_{12} & \bar{Q}_{22} & \bar{Q}_{26} \\ \bar{Q}_{16} & \bar{Q}_{26} & \bar{Q}_{66} \end{bmatrix}_k \begin{Bmatrix} \varepsilon_x \\ \varepsilon_y \\ \gamma_{xy} \end{Bmatrix}$$

$$\begin{Bmatrix} \tau_{yz} \\ \tau_{xz} \end{Bmatrix}_k = \begin{bmatrix} \bar{Q}_{44} & \bar{Q}_{45} \\ \bar{Q}_{45} & \bar{Q}_{55} \end{bmatrix}_k \begin{Bmatrix} \gamma_{yz} \\ \gamma_{xz} \end{Bmatrix} \tag{8}$$

where k denotes the kth lamina and the individual $\bar{Q}_{ij}$ are computed using Jones (1975).

Finally, substituting the expressions for the strains in eqn (5) into the constitutive relations in eqn (8), the stress in the kth lamina of the structural laminate is expressed as:

$$\begin{Bmatrix} \sigma_x \\ \sigma_y \\ \tau_{xy} \end{Bmatrix}_k = \begin{bmatrix} \bar{Q}_{11} & \bar{Q}_{12} & \bar{Q}_{16} \\ \bar{Q}_{12} & \bar{Q}_{22} & \bar{Q}_{26} \\ \bar{Q}_{16} & \bar{Q}_{26} & \bar{Q}_{66} \end{bmatrix}_k \left(\begin{Bmatrix} \varepsilon_x^0 \\ \varepsilon_y^0 \\ \gamma_{xy}^0 \end{Bmatrix} + z \begin{Bmatrix} \kappa_x^0 \\ \kappa_y^0 \\ \kappa_{xy}^0 \end{Bmatrix} + z^2 \begin{Bmatrix} 0 \\ \kappa_y^1 \\ \kappa_{xy}^1 \end{Bmatrix} + z^3 \begin{Bmatrix} \kappa_x^2 \\ \kappa_y^2 \\ \kappa_{xy}^2 \end{Bmatrix} + z^4 \begin{Bmatrix} 0 \\ \kappa_y^3 \\ \kappa_{xy}^3 \end{Bmatrix} \right)$$

$$\begin{Bmatrix} \tau_{yz} \\ \tau_{xz} \end{Bmatrix}_k = \begin{bmatrix} \bar{Q}_{44} & \bar{Q}_{45} \\ \bar{Q}_{45} & \bar{Q}_{55} \end{bmatrix}_k \left(\begin{Bmatrix} \gamma_{yz}^0 \\ \gamma_{xz}^0 \end{Bmatrix} + z^2 \begin{Bmatrix} \kappa_{yz}^1 \\ \kappa_{xz}^1 \end{Bmatrix} \right). \tag{9}$$

The resultant forces and moments and the higher order resultant quantities acting on the laminate are obtained by integrating the stresses in each lamina through the laminate thickness. Thus, for the laminate with N laminae shown in Fig. 2, the resultant forces and
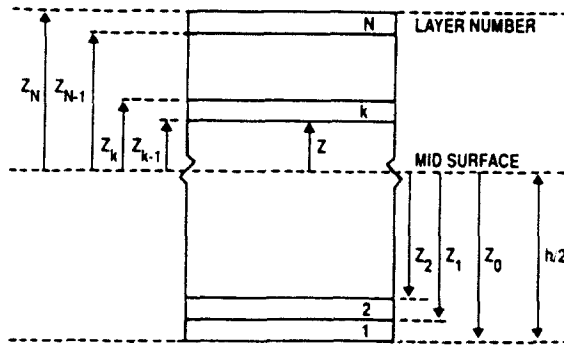
Fig. 2. Geometry of an N-layered laminate.

moments and higher order quantities are:

$$\left\{\begin{matrix} N_1 \\ N_2 \\ N_6 \end{matrix}\right\}, \left\{\begin{matrix} M_1 \\ M_2 \\ M_6 \end{matrix}\right\}, \left\{\begin{matrix} S_1 \\ S_2 \\ S_6 \end{matrix}\right\}, \left\{\begin{matrix} P_1 \\ P_2 \\ P_6 \end{matrix}\right\}, \left\{\begin{matrix} L_1 \\ L_2 \\ L_6 \end{matrix}\right\} = \int_{-h/2}^{h/2} \left\{\begin{matrix} \sigma_x \\ \sigma_y \\ \tau_{xy} \end{matrix}\right\} (1, z, z^2, z^3, z^4)\, dz$$

$$= \sum_{k=1}^{N} \int_{z_{k-1}}^{z_k} \left\{\begin{matrix} \sigma_x \\ \sigma_y \\ \tau_{xy} \end{matrix}\right\}_k (1, z, z^2, z^3, z^4)\, dz$$

$$\left\{\begin{matrix} Q_2 \\ Q_1 \end{matrix}\right\}, \quad \left\{\begin{matrix} R_2 \\ R_1 \end{matrix}\right\} = \int_{-h/2}^{h/2} \left\{\begin{matrix} \tau_{yz} \\ \tau_{xz} \end{matrix}\right\} (1, z^2)\, dz = \sum_{k=1}^{N} \int_{z_{k-1}}^{z_k} \left\{\begin{matrix} \tau_{yz} \\ \tau_{xz} \end{matrix}\right\}_k (1, z^2)\, dz \qquad (10)$$

where $\{N_i\}$ and $\{Q_i\}$ are the resultant forces, $\{M_i\}$ are the resultant moments, and $\{S_i\}$, $\{P_i\}$, $\{L_i\}$, and $\{R_i\}$ are the higher order quantities resulting from the higher order strain-displacement relations.

By substituting eqn (9) into eqn (10), thereby expressing the stresses in terms of the mid-surface displacement quantities and the transformed reduced stiffness matrices, the integration is simplified because the mid-surface values are independent of z and can come out of the integral and summation signs. This allows the following notation to be adopted for the integrated laminate stiffness matrices:

$$(A_{ij}, B_{ij}, D_{ij}, E_{ij}, F_{ij}, G_{ij}, H_{ij}, I_{ij}, J_{ij}) =$$

$$\sum_{k=1}^{N} \begin{bmatrix} \bar{Q}_{11} & \bar{Q}_{12} & \bar{Q}_{16} \\ \bar{Q}_{12} & \bar{Q}_{22} & \bar{Q}_{26} \\ \bar{Q}_{16} & \bar{Q}_{26} & \bar{Q}_{66} \end{bmatrix}_k \int_{z_{k-1}}^{z_k} (1, z, z^2, z^3, z^4, z^5, z^6, z^7, z^8)\, dz \quad i,j = 1,2,6. \quad (11a)$$

For the transverse shear:

$$(A_{ij}, D_{ij}, F_{ij}) = \sum_{k=1}^{N} \begin{bmatrix} \bar{Q}_{44} & \bar{Q}_{45} \\ \bar{Q}_{45} & \bar{Q}_{55} \end{bmatrix}_k \int_{z_{k-1}}^{z_k} (1, z^2, z^4)\, dz \quad i,j = 4,5. \qquad (11b)$$

Now eqn (10) may be written as:

$$
\begin{Bmatrix} N_1 \\ N_2 \\ N_6 \end{Bmatrix}
$$

$$
\begin{Bmatrix} M_1 \\ M_2 \\ M_6 \end{Bmatrix}
$$

$$
\begin{Bmatrix} S_1 \\ S_2 \\ S_6 \end{Bmatrix} =
\begin{bmatrix}
[A_{ij}] & [B_{ij}] & [D_{ij}] & [E_{ij}] & [F_{ij}] \\
[B_{ij}] & [D_{ij}] & [E_{ij}] & [F_{ij}] & [G_{ij}] \\
[D_{ij}] & [E_{ij}] & [F_{ij}] & [G_{ij}] & [H_{ij}] \\
[E_{ij}] & [F_{ij}] & [G_{ij}] & [H_{ij}] & [I_{ij}] \\
[F_{ij}] & [G_{ij}] & [H_{ij}] & [I_{ij}] & [J_{ij}]
\end{bmatrix}
\begin{Bmatrix}
\varepsilon_x^0 \\ \varepsilon_y^0 \\ \varepsilon_{xy}^0 \\
\kappa_x^0 \\ \kappa_y^0 \\ \kappa_{xy}^0 \\
0 \\ \kappa_y^1 \\ \kappa_{xy}^1 \\
\kappa_x^2 \\ \kappa_y^2 \\ \kappa_{xy}^2 \\
0 \\ \kappa_y^3 \\ \kappa_{xy}^3
\end{Bmatrix}
$$

$$
\begin{Bmatrix} P_1 \\ P_2 \\ P_6 \end{Bmatrix}
$$

$$
\begin{Bmatrix} L_1 \\ L_2 \\ L_6 \end{Bmatrix}
$$

$$
i, j = 1, 2, 6
$$

$$
\begin{Bmatrix} Q_2 \\ Q_1 \\ R_2 \\ R_1 \end{Bmatrix} =
\begin{bmatrix}
A_{44} & A_{45} & D_{44} & D_{45} \\
A_{45} & A_{55} & D_{45} & D_{55} \\
D_{44} & D_{45} & F_{44} & F_{45} \\
D_{45} & D_{55} & F_{45} & F_{55}
\end{bmatrix}
\begin{Bmatrix} \gamma_{yz}^0 \\ \gamma_{xz}^0 \\ \kappa_{yz}^1 \\ \kappa_{xz}^1 \end{Bmatrix}
\tag{12}
$$

where the large matrix above is (15×15) and each of its submatrices are (3×3) matrices.

The displacement field, strain-displacement relations, and the laminate resultant quantities in eqn (12) are used in the energy formulation to find the equations of motion and boundary conditions.

The fundamental equation used is Hamilton's Principle (Meirovich, 1967):

$$
\int_{t_1}^{t_2} (\delta T - \delta U - \delta V)\, dt = 0
\tag{13}
$$

where T = kinetic energy, U = strain energy, V = potential energy due to external forces, and δ is the first variation. The derivation of the kinetic energy, strain energy, and potential energy is initially carried out and substituted into eqn (13). The result will be five coupled partial differential equations of motion plus their associated boundary conditions. One obtains double integrals over the domain which contains the five equations of motion. In addition, two line integrals are found. They are the geometric and natural boundary conditions along the four edges of the shell panel. Finally, expressions for the boundary conditions at the four corners are obtained. In the double integral, the variations of the degrees of freedom (δu_0, δv_0, δw, $\delta\psi_x$, and $\delta\psi_y$) are arbitrary and in general are not equal to zero, yielding the five coupled partial differential equations of motion for the panel at any time, t:

the double integral product of δu_0

$$
N_{1,x} + N_{6,y} - \frac{1}{2R} M_{6,y} = I_1 \ddot{u}_0 + I_2 \ddot{\psi}_x - I_3 \ddot{w}_{,x}
$$

product of δv_0

$$N_{2,r}+N_{6,x}+\frac{1}{2R}M_{6,x} = \bar{I}_1\ddot{u}_0+\bar{I}_2\ddot{\psi}_x-\bar{I}_3\ddot{w}_{,r}$$

product of δw

$$-k(P_{1,xx}+P_{2,yy}+2P_{6,xy})+Q_{2,y}+Q_{1,x}+3k(R_{2,y}+R_{1,x})$$

$$-\frac{1}{R}[\bar{N}_2-k(L_{2,yy}+L_{6,xy})]+\bar{N}_1w_{,xx}+2\bar{N}_6w_{,xy}-\bar{N}_2\left[\frac{1}{R}-w_{,yy}\right]$$

$$= \bar{I}_3\ddot{u}_{0,x}+\bar{I}_5\ddot{\psi}_{x,x}+\bar{I}_3\ddot{v}_{0,y}-k^2I_7(\ddot{w}_{,xx}+\ddot{w}_{,yy})+\bar{I}_5\ddot{\psi}_{y,y}+I_1\ddot{w}$$

product of $\delta\psi_x$

$$k(P_{1,x}+P_{6,y})+M_{1,x}+M_{6,y}-3kR_1-Q_1-\frac{1}{R}(S_{6,y}+kL_{6,y}) = \bar{I}_2\ddot{u}_0+\bar{I}_4\ddot{\psi}_x+\bar{I}_5\ddot{w}_{,x}$$

product of $\delta\psi_y$

$$k(P_{2,y}+P_{6,x})+M_{2,y}+M_{6,x}-3kR_2-Q_2-\frac{1}{R}(S_{2,y}+kL_{2,y}) = \bar{I}_2\ddot{v}_0+\bar{I}_4\ddot{\psi}_y-\bar{I}_5\ddot{w}_{,y}$$

<div align="right">(14)</div>

where the following definition for mass moment of inertia is used:

$$(I_1,I_2,I_3,I_4,I_5,I_7) = \int_{h/2}^{h/2}\rho(1,z,z^2,z^3,z^4,z^6)\,dz$$

$$\bar{I}_1 = I_1+\frac{2}{R}I_2$$

$$\bar{I}_2 = I_2+kI_4$$

$$\bar{I}_3 = I_2+\frac{1}{R}I_3+kI_4+\frac{k}{R}I_5$$

$$\bar{I}_3 = -kI_4$$

$$\bar{I}_3 = -kI_4-\frac{k}{R}I_5$$

$$\bar{I}_4 = I_3+2kI_5+k^2I_7$$

$$\bar{I}_5 = -kI_5-k^2I_7.$$

<div align="right">(15)</div>

$\bar{N}_i$ ($i = 1, 2, 6$) are the resultant externally applied quantities assumed to be constant in a buckling analysis and zero in an analysis for natural frequencies as is usually the case, and ρ is the mass density.

These equations of motion will simplify to those of other authors for certain applications. If $R \rightarrow \infty$ in eqns (14) and (15), the equations of motion and boundary conditions reduce to those of a flat plate with parabolic transverse shear and rotary inertia (see Reddy, 1984a,b; Reddy and Liu, 1985; Reddy and Phan, 1985). If the following terms are deleted from the equations of motion in eqn (14):

$$\delta u_0: \quad -\frac{1}{2R}M_{6,x}$$

$$\delta v_0: \quad -\frac{1}{2R}M_{6,x}$$

$$\delta w: \quad \frac{1}{R} k(L_{2,yy} + L_{6,xy})$$

$$\delta \psi_x: \quad -\frac{1}{R}(S_{6,y} + kL_{6,y})$$

$$\delta \psi_y: \quad -\frac{1}{R}(S_{2,y} + kL_{2,y}). \tag{16a-e}$$

the equations of motion reduce to the Donnell-type equations of motion as presented by Reddy and Liu (1985). For $h/R \approx 1/50$, the terms in eqn (16a) are small relative to the other terms in eqn (14), thus establishing the 1/50 limit used by Reddy.

The general equations developed so far need to be tailored to meet the needs of the specific circular cylindrical shell panel to be considered in this paper. First of all, this paper will only consider symmetric laminates: that is, laminates that are symmetric about the mid-surface with respect to both material properties and geometry (fiber orientation angle, θ_k, and thickness, t_k). Therefore, the following stiffness matrices apply:

$$[B_{ij}] = [E_{ij}] = [G_{ij}] = [I_{ij}] = [0]. \tag{17}$$

Additionally, since ρ is constant with respect to z (all laminae have the same density), the inertia terms in eqn (15) may be integrated to yield:

$$I_2 = I_4 = \bar{I}_2 = \bar{I}_3 = 0,$$

$$I_1 = \bar{I}_1 = \rho h,$$

$$I_3 = \rho h^3/12, \quad I_5 + \rho h^5/80, \quad I_7 = \rho h^7/448,$$

$$\bar{I}_2 = \frac{1}{R}\rho h^3/15, \quad \bar{I}_3 = \frac{1}{R}\rho h^3/60, \quad \bar{I}_4 = 17\rho h^3/315, \quad \bar{I}_5 = 4\rho h^3/315. \tag{18}$$

The last simplification concerns the acceleration terms in eqn (14). This paper will consider rotary inertia. In-plane inertia is usually assumed to be small. Consequently, the following in-plane acceleration terms will drop out: $\ddot{u}_0 = \ddot{v}_0 = \ddot{u}_{0,x} = \ddot{v}_{0,y} = 0$.

During the development of the kinetic energy, time-dependent boundaries were ignored because this paper is concerned exclusively with harmonic problems. Assuming harmonic solution forms and applying separation of variables, the five degrees of freedom and their corresponding accelerations may be expressed as:

$$u_0 = u_0(x,y,t) = u_0(x,y) \sin \omega t$$

$$v_0 = v_0(x,y,t) = v_0(x,y) \sin \omega t$$

$$w = w(x,y,t) = w(x,y) \sin \omega t, \quad \ddot{w} = -\omega^2 w(x,y) \sin \omega t = -\omega^2 w$$

$$\psi_x = \psi_x(x,y,t) = \psi_x(x,y) \sin \omega t, \quad \ddot{\psi}_x = -\omega^2 \psi_x(x,y) \sin \omega t = -\omega^2 \psi_x$$

$$\psi_y = \psi_y(x,y,t) = \psi_y(x,y) \sin \omega t, \quad \ddot{\psi}_y = -\omega^2 \psi_y(x,y) \sin \omega t = -\omega^2 \psi_y \tag{19}$$

where ω is the natural frequency of vibration.

If these expressions are substituted into Hamilton's principle, bearing in mind that all the resultant quantities ($\{N_i\}$, $\{M_i\}$, $\{S_i\}$, $\{P_i\}$, $\{L_i\}$, $\{Q_i\}$, and $\{R_i\}$) are functions of the spatial derivatives of u_0, v_0, w, ψ_x, and ψ_y, the term $\sin \omega t$ may be factored out from the entire expression and integrated with respect to time:

$$\int_{t_1}^{t_2} \sin \omega t \, dt = -\frac{1}{\omega} \cos \omega t |_{t_1}^{t_2}. \tag{20}$$

The integrand may be canceled to the right-hand side of the equation, leaving eqn (13) independent of time.

The concepts presented in these paragraphs are now incorporated into Hamilton's Principle, which will be useful in the modified Galerkin method. Equation (13) is partitioned into five equations. Each contains the equation of motion plus the associated boundary condition for a particular degree of freedom (Bowlus *et al.*, 1987; Soldatos, 1987; Whitney, 1984). Equation (13) for u_0 yields:

$$\int_0^b \int_0^a \left(N_{1,x} + N_{6,y} - \frac{1}{2R} M_{6,y} \right) \delta u_0 \, dx \, dy$$

$$+ \int_0^b \bar{N}_1 \delta u_0 |_{x=a}^{x=0} \, dy + \int_0^a \left(\bar{N}_6 - \frac{1}{2R} M_6 \right) \delta u_0 |_{y=b}^{y=0} \, dx = 0. \tag{21}$$

Equation (13) for v_0 yields:

$$\int_0^b \int_0^a \left(I_2 \omega^2 \psi_x - I_3 \omega^2 w_{,x} + N_{2,y} + N_{6,x} + \frac{1}{2R} M_{6,x} \right) \delta v_0 \, dx \, dy$$

$$+ \int_0^b \left(\bar{N}_6 + \frac{1}{2R} M_6 \right) \delta v_0 |_{x=a}^{x=0} \, dy + \int_0^a \bar{N}_2 \delta v_0 |_{y=b}^{y=0} \, dx = 0. \tag{22}$$

Equation (13) for w yields:

$$\int_0^b \int_0^a \left[I_5 \omega^2 (\psi_{x,x} + \psi_{y,y}) - k^2 I_7 \omega^2 (w_{,xx} + w_{,yy}) + I_1 \omega^2 w + Q_{1,x} \right.$$

$$- k(P_{1,xx} + P_{2,yy} + 2P_{6,xy}) + Q_{2,y} + 3k(R_{2,y} + R_{1,x})$$

$$- \frac{1}{R} [\bar{N}_2 - k(L_{2,yy} + L_{6,xy})] + \bar{N}_1 w_{,xx} + 2\bar{N}_6 w_{,xy} - \bar{N}_2 \left(\frac{1}{R} - w_{,yy} \right) \right] \delta w \, dx \, dy$$

$$+ \int_0^b \left(-k(P_{1,x} + 2P_{6,y}) + Q_1 + 3kR_1 + \frac{1}{R} kL_{6,y} + \bar{N}_1 w_{,x} + \bar{N}_6 w_{,y} \right) \delta w |_{x=a}^{x=0} \, dy$$

$$+ \int_0^a \left(-k(P_{2,y} + 2P_{6,x}) + Q_2 + 3kR_2 + \frac{1}{R} k(L_{2,y} + L_{6,x}) \right.$$

$$\left. + \bar{N}_2 w_{,y} + \bar{N}_6 w_{,x} \right) \delta w |_{y=b}^{y=0} \, dx + k \left\{ \left(2P_6 - \frac{1}{R} L_6 \right) \delta w \right\} \Big|_{y=b}^{y=0} \Big|_{x=a}^{x=0} = 0. \tag{23}$$

Equation (13) for ψ_x yields:

$$\int_0^b \int_0^a \left(I_4 \omega^2 \psi_x - I_5 \omega^2 w_{,x} + k(P_{1,x} + P_{6,y}) + M_{1,x} + M_{6,y} - Q_1 \right.$$

$$\left. - 3kR_1 \frac{1}{R}(S_{6,y} + kL_{6,y}) \right) \delta \psi_x \, dx \, dy + \int_0^b (M_1 + 2kP_1) \delta \psi_x |_{x=a}^{x=0} \, dy$$

$$+ \int_0^a \left(M_6 + kP_6 + \frac{1}{R}(-S_6 - kL_6) \right) \delta \psi_x |_{y=b}^{y=0} \, dx = 0. \tag{24}$$

And, finally, eqn (13) for ψ_y yields:

$$\int_0^b \int_0^a \left(I_4\omega^2\psi_y - I_5\omega^2 w_{,y} + k(P_{2,y} + P_{6,x}) + M_{2,y} + M_{6,x} - Q_2 \right.$$

$$\left. -3kR_2\frac{1}{R}(S_{2,y} + kL_{2,y}) \right)\delta\psi_y\, dx\, dy + \int_0^b (M_6 + kP_6)\,\delta\psi_x|_{x=a}^{x=0}\, dy$$

$$+ \int_0^a \left(M_2 + 2kP_2 + \frac{1}{R}(-S_2 - 2kL_2) \right)\delta\psi_x|_{y=b}^{y=0}\, dx = 0. \quad (25)$$

The final step in the development of the equations of motion and boundary conditions is to substitute the resultant quantities to eqn (12) and the strain–displacement relations in eqns (6) and (7) into eqns (21)–(25). [MACSYMA (1985) is used to perform the extensive algebraic manipulations.]

Several observations can be made concerning the five resulting equations. For a flat plate, small deflection theory dictates that bending displacement is completely decoupled from membrane displacement. If the radius of curvature, R, approaches infinity, the five circular cylindrical shell panel equations reduce to those of a flat plate. The two membrane equations for u_0 and v_0 will consist only of extensional stiffness terms, A_{ij}, and spatial derivatives of u_0 and v_0, as expected. Additionally, the three bending equations for w, ψ_x, and ψ_y will consist only of bending and higher order stiffness terms and spatial derivatives of w, ψ_x, and ψ_y. If the higher order stiffness terms are dropped, leaving only A_{ij} and D_{ij}, the three flat plate equations will reduce to those of Bowlus et al. (1985, 1987) and Shames and Dym (1985), which were obtained from the lower order Mindlin transverse shear strain modeling. For R not equal to infinity, membrane and bending displacement are coupled. To find the natural frequencies and buckling loads of the circular cylindrical shell panel, all five equations must be solved simultaneously. This solution will be approximated using the modified Galerkin technique.

Two types of boundary conditions are considered: simply supported conditions on all four edges of the panel and clamped supports.

For the panel simply supported on all sides, the following bending boundary conditions exist:

$$\text{at} \quad x = 0 \quad \text{and} \quad x = a$$
$$w = \psi_y = 0$$

and

$$\text{at} \quad y = 0 \quad \text{and} \quad y = b$$
$$w = \psi_x = 0.$$

As Jones (1975) states, there are four kinds of membrane simply supported boundary conditions possible. An S-2 type condition is used here such that at an edge of the panel, the normal displacement is not zero and the tangential displacement is zero:

$$\text{at} \quad x = 0 \quad \text{and} \quad x = a$$
$$u_0 \neq 0 \quad \text{and} \quad v_0 = 0; \quad \psi_x \neq 0$$

and

$$\text{at} \quad y = 0 \quad \text{and} \quad y = b$$
$$u_0 = 0 \quad \text{and} \quad v_0 \neq 0; \quad \psi_y = 0.$$

Therefore, the admissible functions to be used within the modified Galerkin technique become:

$$\psi_x(x,y) = \sum_{m=1}^{M} \sum_{n=1}^{N} A_{mn} \cos(m\pi x/a) \sin(n\pi y/b)$$

$$\psi_y(x,y) = \sum_{m=1}^{M} \sum_{n=1}^{N} B_{mn} \sin(m\pi x/a) \cos(n\pi y/b)$$

$$w(x,y) = \sum_{m=1}^{M} \sum_{n=1}^{N} C_{mn} \sin(m\pi x/a) \sin(n\pi y/b)$$

$$u_0(x,y) = \sum_{m=1}^{M} \sum_{n=1}^{N} E_{mn} \cos(m\pi x/a) \sin(n\pi y/b)$$

$$v_0(x,y) = \sum_{m=1}^{M} \sum_{n=1}^{N} G_{mn} \sin(m\pi x/a) \cos(n\pi y/b). \tag{26}$$

The single terms associated with the variations of the degrees of freedom are:

$$\delta u_0 \rightarrow \cos(p\pi x/a) \sin(q\pi y/b)$$

$$\delta v_0 \rightarrow \sin(p\pi x/a) \cos(q\pi y/b)$$

$$\delta w \rightarrow \sin(p\pi x/a) \sin(q\pi y/b)$$

$$\delta\psi_x \rightarrow \cos(p\pi x/a) \sin(q\pi y/b)$$

$$\delta\psi_y \rightarrow \sin(p\pi x/a) \cos(q\pi y/b). \tag{27}$$

Notice the indices in eqn (27) are p and q. The single terms that replace the variations of the degrees of freedom govern the number of Galerkin equations. Therefore, the number of terms in each equation is governed by m and n, and the number of equations is governed by p and q.

For the panel clamped on all sides, the following bending boundary conditions exist:

$$\text{at} \quad x = 0 \quad \text{and} \quad x = a$$

$$w = \psi_x = \psi_y = 0$$

and

$$\text{at} \quad y = 0 \quad \text{and} \quad y = b$$

$$w = \psi_x = \psi_y = 0.$$

The membrane boundary conditions will be the same as those in the previous section; from Jones (1975), a C-2 type boundary condition:

$$\text{at} \quad x = 0 \quad \text{and} \quad x = a$$

$$u_0 \neq 0 \quad \text{and} \quad v_0 = 0$$

and

$$\text{at} \quad y = 0 \quad \text{and} \quad y = b$$

$$u_0 = 0 \quad \text{and} \quad v_0 \neq 0.$$

The admissible functions become:

$$\psi_x(x,y) = \sum_{m=1}^{M} \sum_{n=1}^{N} A_{mn} \sin(m\pi x/a) \sin(n\pi y/b)$$

$$\psi_y(x,y) = \sum_{m=1}^{M} \sum_{n=1}^{N} B_{mn} \sin(m\pi x/a) \sin(n\pi y/b)$$

$$w(x,y) = \sum_{m=1}^{M} \sum_{n=1}^{N} C_{mn} \sin(m\pi x/a) \sin(n\pi y/b)$$

$$u_0(x,y) = \sum_{m=1}^{M} \sum_{n=1}^{N} E_{mn} \cos(m\pi x/a) \sin(n\pi y/b)$$

$$v_0(x,y) = \sum_{m=1}^{M} \sum_{n=1}^{N} G_{mn} \sin(m\pi x/a) \cos(n\pi y/b). \tag{28}$$

The single terms associated with the variations of the degrees of freedom are:

$$\delta u_0 \rightarrow \sin(p\pi x/a) \sin(q\pi y/b)$$

$$\delta v_0 \rightarrow \sin(p\pi x/a) \sin(q\pi y/b)$$

$$\delta w \rightarrow \sin(p\pi x/a) \sin(q\pi y/b)$$

$$\delta\psi_x \rightarrow \cos(p\pi x/a) \sin(q\pi y/b)$$

$$\delta\psi_y \rightarrow \sin(p\pi x/a) \cos(q\pi y/b). \tag{29}$$

And, as in the simply supported case, the indices for the single terms are p and q; m and n govern the number of terms per equation, and p and q govern the number of equations.

RESULTS AND DISCUSSION

Several analytical studies were performed. First, a case comparison study with the modified Donnell cylindrical shell panel solutions was carried out. The effects of transverse shear deformation, radius of curvature variation, and rotary inertia were investigated. Finally, the influence of varying the length to span ratio was studied.

Laminated circular cylindrical shell panel properties

The cylindrical shell panel studied in this paper is constructed of graphite–epoxy material and has the following material properties:

$$E_1 = 2.10 \, E+07 \text{ psi}$$

$$E_2 = 1.40 \, E+06 \text{ psi}$$

$$G_{12} = 6.00 \, E+05 \text{ psi}; \quad G_{13} = G_{23} = 0.8 G_{12}$$

$$v_{12} = 0.3$$

$$\rho = 1.42454 \, E-04 \text{ slugs in}^{-3} \, (0.55 \text{ lb in}^{-3}).$$

Two ply lay-ups were investigated: $[0_{50}/90_{50}]$, and $[+45_{50}/\pm45_{50}]$, (both of which for convenience will be referred to as $[0/90]_s$ and $[\pm45]_s$). The latter ply lay-up will introduce more shear stiffness terms into the formulation. The above material properties will be used in all the analyses except for the Donnell comparison investigation.

All panel configurations used in this study displayed excellent frequency and buckling load convergence towards exact answers. This does not prove convergence, but it definitely demonstrates convergence tendencies. The drawback with the Galerkin technique is that in order to obtain extremely accurate answers that require M and N be greater than 10, a great deal of computer resources is required. This higher accuracy requirement has more

application with the buckling loads, since they do not converge as fast as the natural frequencies.

Comparison study with Donnell solution

Reddy and Liu (1985) examined laminated circular cylindrical shell panels using Donnell theory assumptions with parabolic transverse shear modeling. The equations of motion for the circular cylindrical shell panel, eqn (14), will degenerate down to the Donnell equations of motion by dropping the appropriate higher order terms in eqn (16). Reddy found an exact solution to the equations of motion for simply supported boundary conditions using Navier's method. The Navier solution exists only if the following stiffnesses are equal to zero: $A_{i6} = D_{i6} = F_{i6} = H_{i6} = 0$ $(i = 1, 2)$ and $A_{45} = D_{45} = F_{45} = 0$. This restricts his analysis to panels with [0/90], ply lay-ups.

Reddy used different engineering constants in his work than those used in this paper. The following values were used in the comparison:

$$E_1 = 2.1 \, E + 07 \, \text{psi}$$

$$E_2 = 8.4 \, E + 05 \, \text{psi}$$

$$G_{12} = 4.2 \, E + 05 \, \text{psi}$$

$$G_{13} = G_{12}$$

$$G_{23} = 1.68 \, E + 05 \, \text{psi}$$

$$v_{12} = 0.25$$

$$\rho = 1.0 \, \text{slugs in}^{-1} (\text{note an extremely large value}).$$

Table 1 compares Reddy's answers using the Navier solution with those of this paper using the Galerkin technique. Note that Donnell theory limits the maximum h/R ratio to be about 1/50. Table 1 validates the accuracy of the higher order theory as it applies to Donnell-type problems. The excellent agreement between the higher order theory and the Donnell equations is attributed to the h/R region involved. As explained earlier, since the maximum h/R value is 1/50, the higher order terms in eqn (18) approach zero; the higher order equations of motion reduce to Reddy's Donnell equations.

Radius of curvature analysis

The effects of varying the radius of curvature, R (or, equivalently, h/R), is examined in this section. As noted previously, for a flat plate $h/R = 0$, and a membrane completely decouples from bending. The membrane Galerkin equations, those associated with u_0 and v_0, are coupled together, but as a whole are decoupled from the bending Galerkin equations: those associated with w, ψ_x, and ψ_y. As h/R is increased from 0 up to the maximum value of 1/5, membrane and bending couple together, the cylindrical panel becomes deeper and

Table 1. Donnell frequency comparison fundamental frequency (rad s⁻¹)

R (in)	h/R	Navier	Galerkin	Error (%)
$a = b = 100.0$ in				
500.0	0.002	1.86602	1.8697	+0.2
1000.0	0.001	1.52416	1.52458	+0.03
2000.0	0.0005	1.42519	1.42529	+0.007
5000.0	0.0002	1.39585	1.39623	+0.03
$a = b = 10.0$ in				
50.0	0.02	108.4237	108.6415	+0.2
100.0	0.01	108.0571	108.109	+0.05
200.0	0.005	107.9655	107.9753	+0.009
500.0	0.002	107.9655	107.9379	−0.03

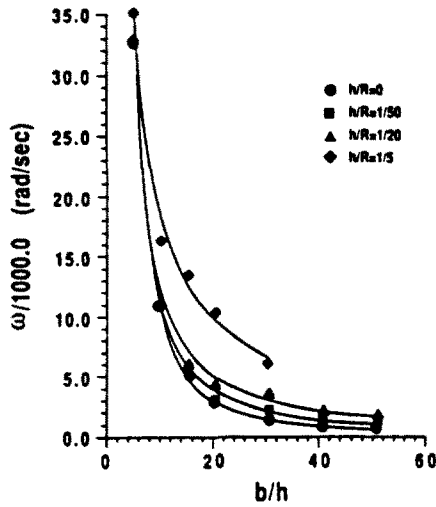Simply supported boundary condition, [0/90], $h = 1.0$ in.

Fig. 3. Curvature effects on frequency. Simply supported boundary, [0/90]$_s$.

stiffer, and the natural frequencies and buckling loads increase. The following specific h/R ratios are investigated:

$$\frac{h}{R} = \begin{cases} 0: & \text{Flat Plate} \\ 1/50: & \text{Donnell Equation Maximum Limit} \\ 1/20: & \text{Intermediate Value} \\ 1/5: & \text{Maximum Limit of Higher Order Theory.} \end{cases}$$

The figures, subsequently shown, are plots of ω or $\bar{N}_1$ vs b/h. The panels have equal length and circumferential dimension; $a/b = 1$, and $M = N = 6$ is used as the degree of accuracy. (The two buckling load plots for $h/R = 1/5$ required $M = N = 8$ for b/h values of 5, 10, and 15 and $M = N = 10$ for b/h values of 20 and 30 to obtain proper convergence.) The circumferential length to thickness ratio (b/h) is varied from 5.0 to 50.0.

The four fundamental frequency plots are shown in Figs 3–6. All curves follow the same basic trends: the frequencies are high at $b/h = 5.0$ and then decrease as the panel gets thinner, approaching constant values asymptotically at b/h values of 40–50. Also, as
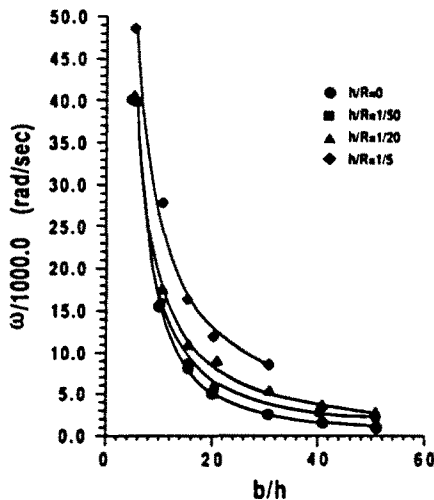

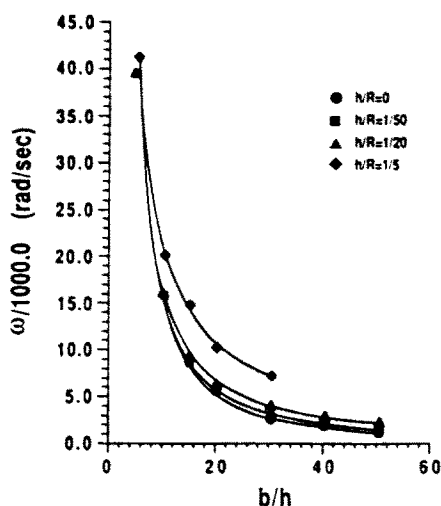Fig. 4. Curvature effects on frequency. Simply supported boundary, [±45]$_s$.

Fig. 5. Curvature effects on frequency. Clamped boundary, [0/90],

expected, the frequencies increase due to membrane and bending coupling as h/R is increased from 0 to 1/5. The effect of this coupling is shown in Table 2 in which panel to flat plate frequency comparisons are made.

With few exceptions, the [±45], laminates generally yield higher frequencies than the [0/90], laminates for both boundary conditions considered. The [±45], laminates have in-plane shear stiffness terms (D_{16}, D_{26}, F_{16}, F_{26}, H_{16}, H_{26}, J_{16}, J_{26}) that account for these higher frequencies. Referring to Figs 3 and 4, for the simply supported boundary condition, the difference in frequency for the two laminates becomes greater as the curvature increases. For $h/R = 0$, the frequencies are about 20% higher for the [±45], laminate for all b/h values. For $h/R = 1/50$, the frequencies are about 20% higher at $b/h = 5$ and are about 50% higher at $b/h = 50$. For $h/R = 1/20$, the frequencies vary from 20% higher to 80% higher, and for $h/R = 1/5$ the frequencies are about 25% higher for all b/h values.

For the clamped boundary condition, the [0/90], laminate yields higher frequencies than the [±45], laminate for flat plates ($h/R = 0$). But, as the curvature increases, the frequencies of the [±45], laminate become greater than those of the [0/90], laminate (see Figs 5 and 6). For $h/R = 150$, the frequencies for both laminates are roughly equal at $b/h = 5$, but the frequencies are about 30% higher for the [±45], laminate at $b/h = 50$. For
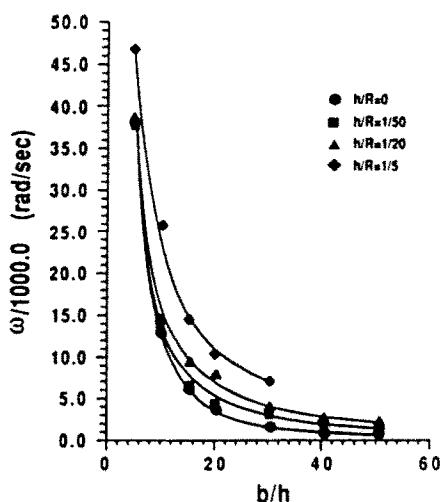

Fig. 6. Curvature effects on frequency. Clamped boundary, [±45],.

Table 2. Frequency coupling effects

	ω/ω_p			
	[0/90],		[±45],	
h/R	$b/h = 10$	$b/h = 30$	$b/h = 10$	$b/h = 30$
Simply supported boundary conditions				
1/5	1.54	4.52	2.02	4.37
1/20	1.04	2.65	1.14	2.48
Clamped boundary conditions				
1/5	1.27	2.67	1.78	3.37
1/20	1.02	1.54	1.10	2.05

ω_p = flat plate natural frequency; $h = 1.0$ in; $a/b = 1$.

$h/R = 1/20$, the frequencies vary from roughly 6% higher to 20% higher, and for $h/r = 1/5$ the frequencies are roughly 30% higher.

Table 2 displays a consistent trend mentioned in the previous two paragraphs; in general, as the curvature of the panel increases, the membrane and bending coupling has a greater effect at larger b/h values. Larger b/h values physically equate to greater arc length around the panel. In fact, for $h/R = 1/5$ at $b/h = 30$ the cylindrical panel is almost a complete cylinder.

For the same ply lay-up, the frequencies for the clamped boundary condition are higher than those for the simply supported boundary condition. For the [0/90], laminate the difference is quite dramatic. For h/R values of 0 and 1/50, the frequencies are 20% higher at $b/h = 5$ and over 100% higher at $b/h = 40$–50. For $h/R = 1/20$ the frequencies are roughly 30% higher for all b/h values, and for $h/R = 1/5$ the frequencies are roughly 20% higher. Figures 4 and 6 show the same trend for the [±45], laminate. The same trends of the frequency plots are evident; high buckling loads at small b/h values, decreasing asymptotically to constant loads at b/h values of 40–50. There are very significant increases in the buckling loads as h/R is increased, and as Table 3 shows, the membrane and bending coupling has a greater effect as the circumferential distance around the panel increases.

The [±45], laminate yields higher buckling loads for the clamped boundary condition than for the simply supported boundary condition for h/R values of 0, 1/50, and 1/20. (See Figs 7 and 8.) The buckling loads are roughly the same for both boundary conditions for $h/R = 1/5$. Similarly, as Table 4 indicates, the [0/90], laminate yields buckling loads for the clamped boundary condition that are upwards of 50% higher than the buckling loads for the simply supported boundary condition, as would be expected.
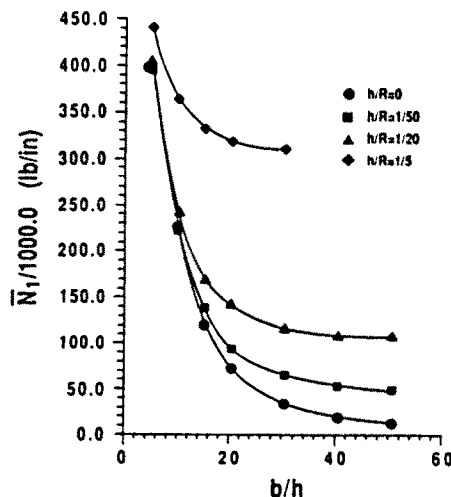

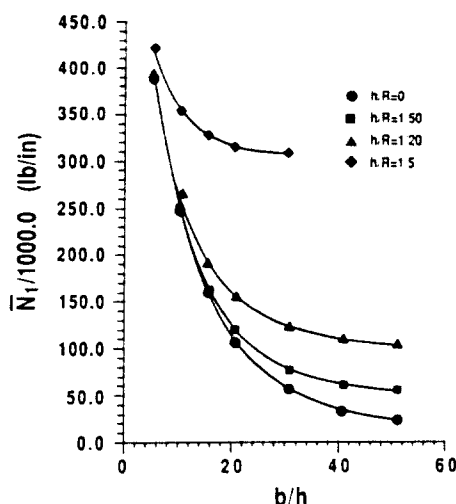Fig. 7. Curvature effects on buckling. Simply supported boundary, [±45],.

Fig. 8. Curvature effects on buckling load. Clamped boundary. [±45],.

Rotary inertia analysis

Another feature of this paper is the incorporation of rotary inertia into the vibration problem. Referring to eqns (14), the following accelerations contribute to the rotary inertia : $\ddot{w}_{,x}$, $\ddot{w}_{,xx}$, $\ddot{w}_{,y}$, $\ddot{w}_{,yy}$, $\ddot{\psi}_x$, $\ddot{\psi}_{x,x}$, $\ddot{\psi}_y$, $\ddot{\psi}_{y,y}$. If rotary inertia is eliminated, the only inertia term left is $I_1\ddot{w}$ on the right-hand side of the equation of motion for w in eqn (14). Likewise, the Galerkin equations all reduce to a single term on the right-hand sides. The end result is a much less populated mass/inertia matrix.

Bowlus (1987) and Palardy and Palazotto (1990) both found rotary inertia to be negligible for the vibration of flat plates modeled with Mindlin transverse shear theory. The results are the same for this paper. Several cases were run for both simply supported and clamped boundary conditions, which included various h/R ratios, ranging from 0 (flat plate) to 1/5, and various a/h (b/h) ratios. The results were all the same. With rotary inertia removed, the fundamental frequencies are only about 0.5% higher. The overall conclusion is that rotary inertia has a negligible effect for first mode analysis. It does become more important for the higher modes, however.

Transverse normal stress considerations

The transverse normal stress, σ_z, was set equal to zero under the assumptions of plane stress constitutive relations. This is a good assumption for most geometries, and is therefore used quite extensively in plate/panel analyses. Some of the geometries analyzed in the previous sections "stretch" the accuracy limitations of the σ_z assumption and warrant specific comments. First, the flat plate is examined.

For flat plates, the validity of assuming $\sigma_z = 0$ is dependent upon the minimum value of a/h (or b/h) chosen. Koiter (1960) states that the transverse normal stress is in general of order h^2/L^2 times the bending stress, and transverse shear strain is h/L times the bending

Table 3. Buckling load coupling effects

	$\bar{N}_1/\bar{N}_{1_F}$			
	Simply supported		Clamped	
h/R	$b/h = 10$	$b/h = 30$	$b/h = 10$	$b/h = 30$
1/5	1.63	9.35	1.43	5.61
1/20	1.08	3.45	1.06	2.22

$\bar{N}_{1_F}$ = flat plate buckling load ; $h = 1.0$ in ; $a/h = 1$; [±45],.

Table 4. Buckling loads for [0/90], laminates

	Critical buckling load (lb in^{-1})	
b/h	Simply supported	Clamped
5	392281.3	454819.2
20	104118.3	195617.0
50	94020.0	134723.6

$R = 20.0$ in; $h = 1.0$ in; $a/b = 1$.

stress, where L is the smallest wavelength of the deformation pattern on the mid-surface. For plates, L is almost always equal to the smallest dimension (a or b). Therefore, for the plate:

$$\sigma_z \approx h^2/a^2(\sigma_x, \sigma_y)$$
$$\tau_{xz}, \tau_{yz} \approx h/a(\sigma_x, \sigma_y). \tag{30}$$

A rule of thumb in classical plate theories is the minimum a/h ratio 10, or $\sigma_z \approx 0.01(\sigma_x, \sigma_y)$. Referring to the previous sections, the minimum a/h (b/h) ratio used is 5; σ_z is roughly 4% of (σ_x, σ_y) and 20% of (τ_{xz}, τ_{yz}), and therefore becomes important for these very thick plate configurations.

Shells incorporate the σ_z approximations with respect to the flat plate, plus an additional accuracy consideration. As Koiter (1960) states, the transverse normal stress is of order h/R times the bending stress. For the shell panel:

$$\sigma_z \approx h/R(\sigma_x, \sigma_y)$$
$$\tau_{xz}, \tau_{yz} \approx h/L(\sigma_x, \sigma_y). \tag{31}$$

When combined together, these equations give:

$$\sigma_z \approx L/R(\tau_{xz}, \tau_{yz}). \tag{32}$$

By the mere fact that the maximum h/R ratio used in this paper is $1/5$, σ_z becomes important because it is in reality roughly 20% of the bending stresses. For the smaller h/R ratios used, the σ_z effect is negligible, except for the regions of small a/h, as explained above.

Using eqn (32), σ_z may be further examined for the h/R ratio of $1/5$. L is not always equal to the dimension of the shell panel; it varies with b/h, and is determined from the mode shape. The longitudinal mode shape generally behaves like that of a flat plate: usually one full sine wave or one half sine wave. The circumferential mode shape varies, depending on the geometry and on the problem (buckling or vibration).

The panel generally buckles into six sine waves in the circumferential direction; $L \approx b/6$ and $L/R \approx b/30$ for $h/R = 1/5$. From eqn (32), σ_z is roughly 15% of (τ_{xz}, τ_{yz}) at $b/h = 5$, where the transverse shear is very prominent. $\sigma_z \approx (\tau_{xz}, \tau_{yz})$ at $b/h = 30$, but the transverse shear here is very low; so, the effect is negligible.

For the vibration problem involving $h/R = 1/5$, there is, in general, only 1–1.5 full sine waves in the circumferential direction; at $L/R \approx 2b/15$, σ_z becomes important at $b/h = 5$ because it is roughly 66% of the transverse shear in a region where the shear is very prominent.

The overall conclusion is that σ_z is important for h/R values of $1/5$ and a/h (b/h) values of 5, especially for the vibration problem. The overall trends displayed by the data, however, are accurate.

Whitney (1987) presents a method that includes σ_z effects and would improve the accuracy for these particular geometries. In his model, the transverse displacement w is a linear function of z and has the form: $w(x, y, z) = w_0(x, y) + z\phi(x, y)$, where $w_0(x, y)$ is the

mid-surface transverse displacement, and $\phi(x,y)$ is an additional degree of freedom that must be included in the constitutive relations and equations of motion.

CONCLUSIONS

A theory applicable to symmetrically laminated anisotropic circular cylindrical shell panels of arbitrary geometries has been developed. The theory includes a through the thickness parabolic transverse shear stress and strain distribution and is valid for $0 \leqslant h/R \leqslant 1.5$. Analytical solutions for the fundamental frequencies. critical buckling loads and the corresponding mode shapes are obtained using the modified Galerkin technique. Simply supported and clamped boundary conditions were investigated. Based upon the analysis, the following conclusions are presented.

The strain–displacement relations are very accurate for $0 \leqslant h/R \leqslant 1.10$. The results were verified against the Donnell solutions for $0 \leqslant h/R \leqslant 1.50$. Since there is no z/R variation in the transverse shear strains. and since σ_z and ε_z are assumed equal to zero, some precision is lost for h/R values of $1/5$. However, the generated results show very logical and consistent trends at this h/R limit, and consequently the theory here is assumed to be a very good approximation.

The modified Galerkin technique proved to be an excellent method for solving the five coupled partial differential equations of motion and boundary conditions. The method converged to exact frequencies very quickly for all geometries. Convergence was slower for the buckling problem, particularly for the clamped boundary condition at $h/R = 1/5$ and high b/h ratios. The method still works for these cases, but at the cost of a great deal of computer time.

Increasing h/R from 0 to $1/5$ increased membrane and bending coupling. and drove the frequencies and buckling loads to higher values for both boundary conditions. For both boundary conditions. the $[\pm 45]_s$ laminates yielded higher frequencies than the $[0/90]_s$ laminates, due to the additional in-plane and transverse shear terms in the former. Both $[\pm 45]_s$ and $[0/90]_s$ laminates yielded higher frequencies for clamped boundary conditions than for simply supported boundary conditions.

Buckling loads behaved differently. The $[\pm 45]_s$ laminates yielded higher buckling loads than the $[0/90]_s$ laminate for simply supported boundary conditions, but $[0/90]_s$ buckling loads are higher than $[\pm 45]_s$ buckling loads for clamped boundary conditions. The $[\pm 45]_s$ laminates have slightly higher buckling loads for clamped versus simply supported boundary conditions, except at $h/R = 1/5$ where the buckling loads for both boundary conditions are roughly equal. Finally, $[0/90]_s$ laminates have much higher buckling loads for clamped boundary conditions than simply supported boundary conditions.

Rotary inertia effects were negligible for all panel configurations examined. Fundamental frequencies were only about 0.5% higher with rotary inertia removed.

REFERENCES

Bert. C. W. and Kumar. M. (1982). Vibration of cylindrical shells of bimodulus composite materials. *J. Sound Vibr.* **81**, 107-121.
Bowlus, J. A. (1985). The determination of the natural frequencies and mode shapes for anisotropic laminated plates including the effects of shear deformation and rotary inertia. M.S. Thesis, AFIT/GA/AA85S-1. School of Engineering. Air Force Institute of Technology (AU), Wright-Patterson AFB, OH.
Bowlus, J. A., Palazotto, A. N. and Whitney, J. M. (1987). Vibration of symmetrically laminated rectangular plates considering deformation and rotary inertia. *AIAA Jl* **25**, 1500 1511.
Dennis. S. T. and Palazotto. A. N. (1989). Transverse shear deformation with orthotropic cylindrical pressure vessels using a higher-order shear theory. *AIAA Jl* **27**, 1441 1447.
Dennis, S. T. and Palazotto. A. N. (1990). Large displacement and rotational formulation for laminated shells including parabolic transverse shear. *Int. J. Nonlinear Mech.* **25**, 67 85.
Jones. R. M. (1975). *Mechanics of Composite Materials*. Hemisphere. New York.
Koiter, W. T. (1960). A consistent first approximation in the general theory of thin elastic shells. *Proc. Symp. on Theory of Thin Elastic Shells*, pp. 12 33. North Holland. Amsterdam.

Meirovitch, L. (1967). *Analytical Methods in Vibrations*. MacMillan, New York.

Mindlin, R. D. (1951). Influence of rotary inertia and shear on flexural motions of isotropic elastic plates. *J. Appl. Mech.* **18**, 31–38.

Palardy, R. F. and Palazotto, A. N. (1990). Buckling and vibration of composite plates using the Levy method. *J. Compos. Struct.* **14**, 63–86.

Reddy, J. N. (1984a). *Energy and Variational Methods in Applied Mechanics*. John Wiley, New York.

Reddy, J. N. (1984b). A simple higher-order theory for laminated composite plates. *J. Appl. Mech.* **51**, 745–752.

Reddy, J. N. and Liu, C. F. (1985). A higher-order shear deformation theory of laminated elastic shell. *Int. J. Engng Sci.* **23**, 319–330.

Reddy, J. N. and Phan, N. D. (1985). Stability and vibration of isotropic, orthotropic, and laminated plates according to a higher order shear deformation theory. *J. Sound Vibr.* **98**, 157–170.

Reissner, E. (1945). The effect of transverse shear deformation on the bending of elastic plates. *J. Appl. Mech. ASME* **55**, 69–77.

Saada, A. (1974). *Elasticity: Theory and Applications*. Pergamon Press, New York.

Shames, I. H. and Dym, C. D. (1985). *Energy and Finite Element Methods in Structural Mechanics*. McGraw-Hill, New York.

Soldatos, K. P. (1987). Buckling of axially compressed antisymmetric angle-ply laminated circular cylindrical panels according to a refined shear deformable shell theory. *ASME PVP* **124**, 63–71.

Vax Unix MACSYMA Reference Manual (1985). Massachusetts Institute of Technology, Symbolics, Inc.

Whitney, J. M. (1984). Buckling of anisotropic laminated cylindrical plates. *AIAA Jl* **22**, 1641–1645.

Whitney, J. M. (1987). *Structural Analysis of Laminated Anisotropic Plates*. Technomic, Lancaster, PA.